Astronomy & Astrophysics

L{ETTER TO THE} E{DITOR}

B field in OB stars (BOB): The outstandingly strong magnetic field in the evolved He-strong star CPD −62° 2124[⋆]

N. Castro[1,2], L. Fossati[3,2], S. Hubrig[4], S. P. Järvinen[4], N. Przybilla[5], M.-F. Nieva[5], I. Ilyin[4], T. A. Carroll[4], M. Schöller[6], N. Langer[2], F. R. N. Schneider[7], S. Simón-Díaz[8,9], T. Morel[10], K. Butler[11], and the BOB collaboration

[1] Department of Astronomy, University of Michigan, 1085 S. University Avenue, Ann Arbor, MI 48109-1107, USA
     e-mail: ncastror@umich.edu
[2] Argelander-Institut für Astronomie der Universität Bonn, Auf dem Hügel 71, 53121 Bonn, Germany
[3] Space Research Institute, Austrian Academy of Sciences, Schmiedlstrasse 6, 8042 Graz, Austria
[4] Leibniz-Institut für Astrophysik Potsdam (AIP), An der Sternwarte 16, 14482 Potsdam, Germany
[5] Institut für Astro- und Teilchenphysik, Universität Innsbruck, Technikerstr. 25/8, 6020 Innsbruck, Austria
[6] European Southern Observatory, Karl-Schwarzschild-Str. 2, 85748 Garching bei München, Germany
[7] Department of Physics, University of Oxford, Denys Wilkinson Building, Keble Road, Oxford OX1 3RH, UK
[8] Instituto de Astrofísica de Canarias, 38200 La Laguna, Tenerife, Spain
[9] Universidad de La Laguna, 38205 La Laguna, Tenerife, Spain
[10] Space Sciences, Technologies and Astrophysics Research (STAR) Institute, Université de Liège, Quartier Agora,
     Allée du 6 Août 19c, Bât. B5C, 4000 Liège, Belgium
[11] Universitäts-Sternwarte München, Scheinerstr. 1, 81679 München, Germany

ABSTRACT

The origin and evolution of magnetism in OB stars is far from being well understood. With approximately 70 magnetic OB stars known, any new object with unusual characteristics may turn out to be a key piece of the puzzle. We report the detection of an exceptionally strong magnetic field in the He-strong B2IV star CPD −62° 2124. Spectropolarimetric FORS2 and HARPSpol observations were analysed by two independent teams and procedures, concluding on a strong longitudinal magnetic field of approximately 5.2 kG. The quantitative characterisation of the stellar atmosphere yields an effective temperature of 23 650 ± 250 K, a surface gravity of 3.95 ± 0.10 dex and a surface helium fraction of 0.35 ± 0.02 by number. The metal composition is in agreement with the cosmic abundance standard, except for Mg, Si and S, which are slightly non-solar. The strong and broad ($\sim$300 km s^{-1}) disc-like emission displayed by the Hα line suggests a centrifugal magnetosphere supported by the strong magnetic field. Our results imply that CPD −62° 2124 is an early B-type star hosting one of the strongest magnetic fields discovered to date, and one of the most evolved He-strong stars known, with a fractional main-sequence lifetime of approximately 0.6.

Key words. stars: atmospheres – stars: evolution – stars: magnetic field – stars: massive – stars: individual: CPD-62 2124

1. Introduction

The recent efforts invested in the search for magnetic fields in the most massive O- and B-type stars have provided more than 70 confirmed magnetic detections (e.g. Petit et al. 2013; Alecian et al. 2014; Fossati et al. 2014; Hubrig et al. 2014a; Neiner et al. 2014; Castro et al. 2015) and a magnetic incidence rate of approximately 7% (Wade et al. 2014; Fossati et al. 2015b; Grunhut et al. 2016; Schöller et al. 2017). Any new addition to the scarce number of known magnetic stars, especially objects with unusual characteristics, has the potential to improve our understanding of the origin of magnetism and its role in stellar structure and evolution (Langer 2012; Petermann et al. 2015), as well as in the characteristics of the circumstellar environment (Petit et al. 2013) and spectral features linked to the magnetic field (e.g. Of?p stars; Nazé et al. 2010). Detections of strong (i.e. longitudinal field larger than 1 kG) magnetic fields have been reported in the literature among He-strong stars (e.g. Landstreet & Borra 1978; Borra & Landstreet 1979; Bohlender 1988; Bagnulo et al. 2006; Hubrig et al. 2015), pointing out He-strong stars as a sub-class of strong magnetic early B-type stars.

Within the context of the "B fields in OB stars" (BOB) collaboration (Morel et al. 2014, 2015; Hubrig et al. 2014a, 2015; Fossati et al. 2015b; Schöller et al. 2017), here we report the detection of an exceptionally strong magnetic field in the He-strong B2IV star CPD −62° 2124 (V = 11.04 mag; Drilling 1981; Walborn 1983; Zboril et al. 1997; Renson & Manfroid 2009). The star was observed using two different instruments (Sect. 2) and the magnetic field was detected and confirmed by independent teams employing different techniques (Sect. 3). Section 4 presents the stellar atmospheric and chemical abundance analyses, and gives the derived stellar evolution properties. The results are discussed and conclusions are drawn in Sect. 5.

2. Observations

We observed CPD −62° 2124 on 17th March, 2015, using the FORS2 low-resolution spectropolarimeter (Appenzeller et al. 1998) attached to the ESO/VLT UT1 (Antu) of the Paranal Observatory (Chile). The data were taken with a slit width of 0.4″ and the grism 600B. This setting led to a resolving power of approximately 1700 and a wavelength coverage from 3250–6215 Å. Eight consecutive exposures of 600 s were carried out with a total exposure time of 4800 s. More details on

---

⋆ Based on observations made with ESO telescopes at the La Silla and Paranal observatories under programme ID 191.D-0255(G,I).

the instrument settings and exposure sequence are provided by Hubrig et al. (2014a; see also Fossati et al. 2015b).

We also observed CPD −62° 2124 with the HARPSpol spectropolarimeter (Snik et al. 2011; Piskunov et al. 2011) attached to the ESO 3.6 m telescope of La Silla Observatory (Chile) on 4th June 2015. The HARPSpol data cover the spectral range 3780–6910 Å with a resolving power of ≈115 000. Four exposures of 1800 s each were obtained, rotating the quarter-wave retarder plate by 90° after each exposure (further details are reported by e.g. Hubrig et al. 2014a; Fossati et al. 2015a). The final Stokes I spectrum has a signal-to-noise ratio per pixel of approximately 70, calculated at 5000 Å.

## 3. The strong surface magnetic field of CPD −62° 2124

The FORS2 data were reduced and analysed using independent pipelines by the Bonn (Fossati et al. 2015b) and Potsdam (Hubrig et al. 2014b) teams. The obtained longitudinal magnetic field values ($\langle B_z \rangle$) are listed in Table 1. Figure A.1 shows the output of the Bonn pipeline, where the strong surface longitudinal magnetic field of CPD −62° 2124 is revealed by the slope in the top-right panel (see Potsdam outcome in Schöller et al. 2017).

Both pipelines led to a strong magnetic field detection using either the hydrogen lines or the whole spectrum. Nonetheless, there is a difference of approximately 600 G between the measurements based on the hydrogen lines, whereas the values are consistent within the errors when the whole spectrum is considered. Such discrepancies for strongly magnetic stars are not uncommon (see Landstreet et al. 2014; Fossati et al. 2015b).

The subsequent HARPSpol spectrum of CPD −62° 2124 confirmed the presence of a strong magnetic field. The HARPSpol data were independently reduced and analysed using different techniques by the Bonn and Potsdam groups, as described in previous BOB works (Hubrig et al. 2014a; Przybilla et al. 2016).

The $\langle B_z \rangle$ values, derived from the HARPSpol spectra, were estimated adopting two techniques: the least-squares deconvolution technique (LSD; Donati et al. 1997; Kochukhov et al. 2010) and the single value decomposition technique (SVD; Carroll et al. 2012). We derived the $\langle B_z \rangle$ values considering 90 metal lines and ignoring He lines because of their large width and the inhomogeneous surface distribution that biases the magnetic field measurements (see Table 1). Each analysis of the Stokes V spectra led to a definite detection of the magnetic field, while, as seen in Fig. 1, non-detections were obtained from the diagnostic null profiles (see Bagnulo et al. 2009, for details).

The LSD analysis of the rather noisy HARPS observations carried out by the Bonn group resulted in a $\langle B_z \rangle$ value of approximately 5.2 kG. However, the LSD and SVD applied to the spectra reduced by the Potsdam group led to $\langle B_z \rangle$ values of the order of 3–3.5 kG. On the other hand, if the Potsdam group uses the spectra extracted measurements of the Bonn group, the results obtained for SVD and LSD, 5.1 ± 0.3 kG and 5.4 ± 0.3 kG, respectively, match the Bonn result well. Since the Potsdam analysis is based on two-dimensional spectra extracted using the ESO HARPS pipeline. It is very likely that the pipeline spectrum extraction is sensitive to the noise level in the observed spectra, which in the case of our HARPS observations is rather high compared to our previous observations with this instrument, and for which we have never encountered a similar problem (Hubrig et al. 2014a; Castro et al. 2015; Przybilla et al. 2016). The presence of the remarkably strong magnetic field is also supported by the results of our preliminary reduction of new
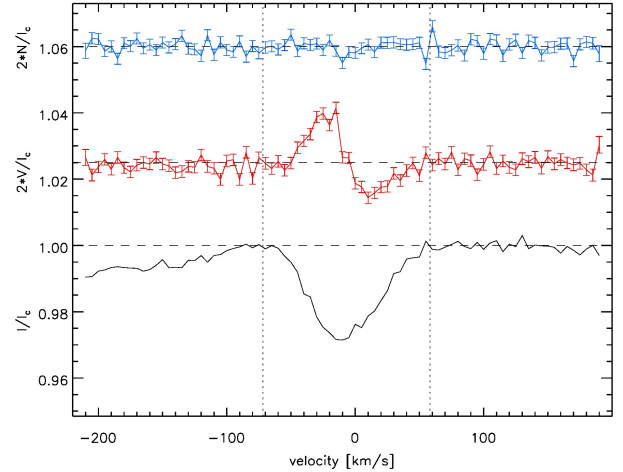
Fig. 1. LSD profiles of Stokes I, V and N parameters obtained for CPD −62° 2124 by the Bonn group. The vertical dotted lines indicate the velocity range adopted for the determination of the detection probability and $\langle B_z \rangle$ value. The Stokes V and N profiles have been shifted upwards by an arbitrary value and expanded by a factor of two.

Table 1. Longitudinal magnetic field ($\langle B_z \rangle$) values of CPD −62° 2124 obtained from the FORS2 and HARPSpol spectra.

FORS 2			
Group	Date/MJD	Lines	$\langle B_z \rangle$ [G]
Bonn	17-Mar.-2015/ 57 099.21385	H lines	5220 ± 120
		Whole spectrum	4340 ± 60
Potsdam		H lines	4640 ± 130
		Whole spectrum	4530 ± 100
HARPSpol			
Group	Date/MJD	Lines	$\langle B_z \rangle$ V [G]
Bonn (LSD)	04-Jun.-2015/ 57 177.95220	Metals	5200 ± 400
Potsdam (SVD)			5100 ± 300
Potsdam (LSD)			5400 ± 300

Notes. Column 1 indicates the group that performed the data reduction and analysis. The technique used for the analysis of the HARPSpol spectra is given in brackets. Column 2 lists the observing date. Column 3 gives the considered spectral regions (see Sect. 3 for details).

multi-epoch FORS 2 observations (Hubrig et al. in prep.) of this star, which indicate that the magnetic field is always stronger than 4 kG.

With a $\langle B_z \rangle$ of approximately 5.2 kG, the magnetic field of CPD −62° 2124 is one of the strongest measured so far in stars of the upper main-sequence. Follow-up observations of CPD −62° 2124 will constrain its magnetic field strength, its time dependence and geometry and the stellar rotation period.

4. Stellar parameters and chemical abundances

CPD −62° 2124 is the second He-strong star for which the BOB consortium discovered the presence of a magnetic field and derived the stellar parameters. Przybilla et al. (2016) presented the magnetic field detection and parameters for CPD −57° 3509, which is also a He-strong B2IV star, though with a weaker magnetic field ($\langle B_z \rangle \approx 1.1$ kG) compared to that of CPD −62° 2124.

The average projected rotational ($\upsilon \sin i$) and macroturbulence (ζ) velocities of 35 ± 5 km s^{-1} and 40 ± 5 km s^{-1}, respectively, were obtained from the HARPSpol

Stokes *I* spectrum employing the IACOB-BROAD code (Simón-Díaz & Herrero 2014). The velocities were independently derived using the tools described by Nieva & Przybilla (2012). The two techniques employed approximately 30 and 90 spectral lines, respectively, belonging to nine different chemical elements (see Table 2). The derived ζ velocity is approximately 1.5 times higher than the average for stars of similar spectral type (Simón-Díaz et al. 2017). Magnetic splitting could affect the spectral lines, leading to a higher macroturbulence value. Pulsations found in similar B-type stars could also lead to higher macroturbulence (Aerts et al. 2014).

The atmospheric characterisation of CPD −62° 2124 was carried out using the hybrid non-LTE approach described by Nieva & Przybilla (2007) and the same strategy as followed for CPD −57° 3509. A description of the technique, atomic models and limitations is given by Przybilla et al. (2016), with the difference being that in this analysis we did not consider the hydrogen Balmer lines that are contaminated by circumstellar emission (see Sect. 5). The atmospheric parameters were obtained considering the collective ionisation equilibria for elements for which lines are presented in the HARPSpol spectrum: He I/II, C II/III, Si II/III/IV, O I/II and S II/III, which results in small uncertainties. Table 2 lists the obtained parameters and chemical abundances, comparing them to the cosmic abundance standard (CAS; Nieva & Przybilla 2012; Przybilla et al. 2013). Figure B.1 shows a comparison between the HARPSpol spectrum and the best fitting synthetic model. A good match is obtained with only small asymmetries/peculiarities present, suggesting that chemical inhomogeneities, such as spots on the surface, are dominating. Exceptions being the Balmer lines, which show an important contribution from the circumstellar material. Zboril et al. (1997), by fitting the Balmer lines, derived a higher effective temperature of 26 000 K and surface gravity of 4.2 dex. The authors mention the emission in the Balmer lines as a possible source of uncertainty. In addition, their neglect of metal lines and non-LTE effects contributes to the differences.

The lines from the investigated chemical species react differently to magnetic broadening (which is unaccounted for in our modelling). While an overall systematic reduction of abundance values can be expected, the effect should be covered by the 1σ-uncertainties (see Table 2), as implied by the good match of model and observation and the only slightly higher uncertainties with respect to standard B-stars, in the CAS study for example.

The stellar mass (M), radius (R), luminosity (L), evolutionary age (τ) and fractional main-sequence lifetime (τ/τ_{MS}) were derived from comparisons with stellar evolutionary tracks by Ekström et al. (2012) and Brott et al. (2011; Table 2). When considering the rotating stellar evolutionary tracks by Brott et al. (2011), we inferred stellar parameters using the BONNSAI[1] tool (Schneider et al. 2014). In the relevant mass range, the small differences between the two sets of tracks are attributed mainly to differences in the adopted overshooting parameters (see e.g. Castro et al. 2014). Note that the evolutionary tracks were computed assuming solar abundances, though we expect this to have a small effect because the He overabundance should be confined to the outermost layers only, implying no influence on the evolution of the star (Przybilla et al. 2016).

5. Discussion and conclusion

On the basis of the available information, and assuming a dipolar magnetic field geometry, the lower limit on the dipolar magnetic field strength (B_d), calculated using the relations

---

[1] http://www.astro.uni-bonn.de/stars/bonnsai

Table 2. Parameters and elemental abundances of CPD −62° 2124.

Atmospheric parameters:		
T_{eff} [K]	$23\,650 \pm 250$	
$\log g$ [cgs]	3.95 ± 0.10	
y [number fraction]	0.35 ± 0.02	
ξ [km s^{-1}]	2 ± 1	
$v \sin i$ [km s^{-1}]	35 ± 5	
ζ [km s^{-1}]	40 ± 5	
Non-LTE metal abundances:		
	CPD −62° 2124	CAS
$\log$ (C/H) + 12	8.29 ± 0.06 (7)	8.33 ± 0.04
$\log$ (N/H) + 12	7.72 ± 0.14 (17)	7.79 ± 0.04
$\log$ (O/H) + 12	8.69 ± 0.15 (27)	8.76 ± 0.05
$\log$ (Ne/H) + 12	8.15 ± 0.09 (4)	8.09 ± 0.05
$\log$ (Mg/H) + 12	7.37 (1)	7.56 ± 0.05
$\log$ (Al/H) + 12	6.19 ± 0.06 (5)	6.30 ± 0.07
$\log$ (Si/H) + 12	7.77 ± 0.10 (10)	7.50 ± 0.05
$\log$ (S/H) + 12	7.38 ± 0.09 (7)	7.14 ± 0.06
$\log$ (Fe/H) + 12	7.59 ± 0.12 (7)	7.52 ± 0.03
Fundamental parameters:		
	Ekström et al. (2012)	Brott et al. (2011)
$M/M_\odot$	10.0 ± 0.4	$9.8^{+0.6}_{-0.4}$
$R/R_\odot$	5.8 ± 0.9	$5.05^{+0.76}_{-0.66}$
$\log L/L_\odot$	3.98 ± 0.11	$3.88^{+0.11}_{-0.13}$
τ [Myr]	$16.4^{+0.9}_{-2.5}$	$14.54^{+1.04}_{-2.12}$
τ/τ_{MS}	$0.65^{+0.04}_{-0.10}$	$0.59^{+0.11}_{-0.12}$

Notes. The number of lines considered for the determination of the chemical abundances is given in brackets. The cosmic abundance standard (CAS, Nieva & Przybilla 2012) in the solar neighbourhood is given for reference, along with data for Al and S from Przybilla et al. (2013).
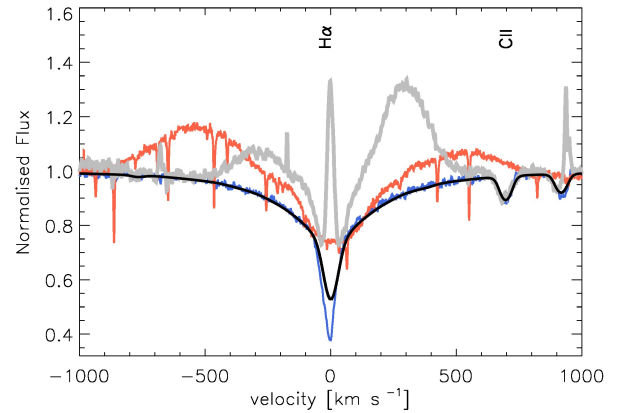
Fig. 2. Normalised HARPS spectrum of CPD −62° 2124 (grey solid line) in the Hα spectral region. The synthetic photospheric CPD −62° 2124 spectrum is also shown (black solid line), together with the HARPSpol spectrum of the He-strong stars CPD −57° 3509 (blue line, Przybilla et al. 2016) and that of HD 37479 (red line, e.g. Oksala et al. 2012). The spectrum of HD 37479 was obtained within the context of the IACOB project[2] (Simón-Díaz et al. 2011, 2015). The narrow central emission in the CPD −62° 2124 spectrum is of nebular origin.

of Preston (1967) and assuming a limb darkening coefficient of 0.3 (see Claret & Bloemen 2011), is equal to 18.3 kG.

Note that Petit et al. (2013) adopted a more conservative limb darkening coefficient of 0.6, under this approximation CPD −62° 2124's dipolar magnetic field strength is 17.2 kG. Among the known magnetic massive stars, only NGC 1624-2 ($\langle B_z \rangle = 5.35$ kG; Wade et al. 2012) and the He-strong star

---

[2] http://vivaldi.ll.iac.es:8080/iacob/jsp/search.jsp

HD 64740 ($\langle B_z \rangle \approx 4.8$ kG; Petit et al. 2013) host a magnetic field with a strength comparable to that of CPD −62° 2124.

From the measured $\upsilon \sin i$ value, inferred stellar radius and mass, and assuming an equator-on view, we obtain a maximum rotation period of 7.3 days and an upper limit on the Keplerian corotation radius of 6.7 stellar radii. Adopting $B_d = 18.3$ kG, we obtain lower limits on the Alfvén radius of approximately 35.2 stellar radii. For these calculations we adopted the stellar parameters obtained from BONNSAI (including a mass-loss rate of $1.6 \times 10^{-9} M_\odot$ yr^{-1}) and a terminal velocity of 700 km s^{-1} (Oskinova et al. 2011). Following the results of Petit et al. (2013), CPD −62° 2124 should have a centrifugal magnetosphere.

The Hα line profile (Fig. 2) supports the presence of a disc-like centrifugal magnetosphere. The line presents a central absorption component and line-wing emissions on both sides of the Hα line extending up to approximately ± 300 km s^{-1}. The presence of similar Hα emission wings has been reported for other strongly magnetic He-strong stars, such as HD 23478 ($\langle B_z \rangle = 1.5$ kG; Hubrig et al. 2015) and HD 37479 (σ Ori E, $\langle B_z \rangle = 2.4$ kG; Oksala et al. 2012), for example. Despite the similarities between the He-strong stars CPD −62° 2124 and CPD −57° 3509, the latter does not show any spectral feature indicative of circumstellar material (see Fig. 2), although on theoretical grounds it could also host a centrifugal magnetosphere ($\langle B_z \rangle = 1.1$ kG; Przybilla et al. 2016). CPD −62° 2124 therefore provides a further empirical constrain on the physical conditions (e.g. stellar evolutionary stage, rotation and magnetic field strength) that need to be met for a magnetic star to host and display the signature of a magnetosphere at optical wavelengths (ud-Doula & Owocki 2002; Shultz et al. 2014). The large circumstellar velocities, particularly compared to the low measured $\upsilon \sin i$ value, may be due to fact that the emission occurs at large stellar radius in conjunction with rigid rotation due to magnetic coupling. In this scenario, the centrifugal magnetosphere peaks at approximately 8.5 stellar radii.

Based on the B_d value of 18.3 kG and assuming flux conservation as the only mechanism affecting the magnetic field strength, CPD −62° 2124 would have had a dipolar magnetic field strength on the zero-age main-sequence (ZAMS) larger than 34.1 kG (the evolutionary tracks of Brott et al. 2011 give a ZAMS radius of $3.7 R_\odot$). These values could be even larger, if one accounts for the possibility of magnetic field decay (Fossati et al. 2016). Following the formulation of Ud-Doula et al. (2009) and Petit et al. (2013), and using the stellar parameters from BONNSAI, a gyration constant of 0.04 (Fossati et al. 2016) and the mass-loss rate, terminal velocity and maximum rotation period mentioned earlier in this section, we obtain an upper limit on the spin-down age (the time required to spin down a star from critical rotation to the current rotation rate) of approximately 0.8 Myr, which is much smaller than the age of the star, suggesting that the magnetic field might have been generated during the main-sequence evolution, possibly following a merger event.

We derived a chemical composition consistent with the CAS (Nieva & Przybilla 2012; Przybilla et al. 2013) and only silicon, sulphur and magnesium (magnesium abundance based only on Mg II 4481 Å) show small deviations from abundances typical of nearby B stars (off by ≈ 0.25 dex). The large helium abundance ($y = 0.35 \pm 0.02$ number fraction) is the only strong peculiarity derived from the abundance analysis. CPD −62° 2124 adds to the continuously increasing group of He-strong stars for which a magnetic field has been detected. This further supports the hypothesis (Borra & Landstreet 1979) that the rise of a surface He overabundance is closely related to the presence of strong surface magnetic fields.

References

Aerts, C., Simón-Díaz, S., Groot, P. J., & Degroote, P. 2014, A&A, 569, A118
Alecian, E., Kochukhov, O., Petit, V., et al. 2014, A&A, 567, A28
Appenzeller, I., Fricke, K., Fürtig, W., et al. 1998, The Messenger, 94, 1
Bagnulo, S., Landstreet, J. D., Mason, E., et al. 2006, A&A, 450, 777
Bagnulo, S., Landolfi, M., Landstreet, J. D., et al. 2009, PASP, 121, 993
Bohlender, D. A. 1988, Ph.D. Thesis, The university of Western Ontario, Canada
Borra, E. F., & Landstreet, J. D. 1979, ApJ, 228, 809
Brott, I., de Mink, S. E., Cantiello, M., et al. 2011, A&A, 530, A115
Carroll, T. A., Strassmeier, K. G., Rice, J. B., & Künstler, A. 2012, A&A, 548, A95
Castro, N., Fossati, L., Langer, N., et al. 2014, A&A, 570, L13
Castro, N., Fossati, L., Hubrig, S., et al. 2015, A&A, 581, A81
Claret, A., & Bloemen, S. 2011, A&A, 529, A75
Donati, J.-F., Semel, M., Carter, B. D., Rees, D. E., & Collier Cameron, A. 1997, MNRAS, 291, 658
Drilling, J. S. 1981, ApJ, 250, 701
Ekström, S., Georgy, C., Eggenberger, P., et al. 2012, A&A, 537, A146
Fossati, L., Zwintz, K., Castro, N., et al. 2014, A&A, 562, A143
Fossati, L., Castro, N., Morel, T., et al. 2015a, A&A, 574, A20
Fossati, L., Castro, N., Schöller, M., et al. 2015b, A&A, 582, A45
Fossati, L., Schneider, F. R. N., Castro, N., et al. 2016, A&A, 592, A84
Grunhut, J. H., Wade, G. A., Neiner, C., et al. 2016, MNRAS, submitted [arXiv:1610.07895]
Hubrig, S., Fossati, L., Carroll, T. A., et al. 2014a, A&A, 564, L10
Hubrig, S., Schöller, M., & Kholtygin, A. F. 2014b, MNRAS, 440, 1779
Hubrig, S., Schöller, M., Fossati, L., et al. 2015, A&A, 578, L3
Kochukhov, O., Makaganiuk, V., & Piskunov, N. 2010, A&A, 524, A5
Landstreet, J. D., & Borra, E. F. 1978, ApJ, 224, L5
Landstreet, J. D., Bagnulo, S., & Fossati, L. 2014, A&A, 572, A113
Langer, N. 2012, ARA&A, 50, 107
Morel, T., Castro, N., Fossati, L., et al. 2014, The Messenger, 157, 27
Morel, T., Castro, N., Fossati, L., et al. 2015, in IAU Symp., 307, 342
Nazé, Y., Ud-Doula, A., Spano, M., et al. 2010, A&A, 520, A59
Neiner, C., Tkachenko, A., & MiMeS Collaboration 2014, A&A, 563, L7
Nieva, M. F., & Przybilla, N. 2007, A&A, 467, 295
Nieva, M.-F., & Przybilla, N. 2012, A&A, 539, A143
Oksala, M. E., Wade, G. A., Townsend, R. H. D., et al. 2012, MNRAS, 419, 959
Oskinova, L. M., Todt, H., Ignace, R., et al. 2011, MNRAS, 416, 1456
Petermann, I., Langer, N., Castro, N., & Fossati, L. 2015, A&A, 584, A54
Petit, V., Owocki, S. P., Wade, G. A., et al. 2013, MNRAS, 429, 398
Piskunov, N., Snik, F., Dolgopolov, A., et al. 2011, The Messenger, 143, 7
Preston, G. W. 1967, ApJ, 150, 547
Przybilla, N., Nieva, M. F., Irrgang, A., & Butler, K. 2013, in EAS Pub. Ser., 63, 13
Przybilla, N., Fossati, L., Hubrig, S., et al. 2016, A&A, 587, A7
Renson, P., & Manfroid, J. 2009, A&A, 498, 961
Schneider, F. R. N., Langer, N., de Koter, A., et al. 2014, A&A, 570, A66
Schöller, M., Hubrig, S., Fossati, L., et al. 2017, A&A, in press, DOI: 10.1051/0004-6361/201628905
Shultz, M., Wade, G., Rivinius, T., Townsend, R., & the MiMeS Collaboration 2014, ArXiv e-prints [arXiv:1411.2542]
Simón-Díaz, S., & Herrero, A. 2014, A&A, 562, A135
Simón-Díaz, S., Castro, N., Garcia, M., & Herrero, A. 2011, in IAU Symp., 272, 310
Simón-Díaz, S., Negueruela, I., Maíz Apellániz, J., et al. 2015, in Highlights of Spanish Astrophysics VIII, 576
Simón-Díaz, S., Godart, M., Castro, N., et al. 2017, A&A, 597, A22
Snik, F., Kochukhov, O., Piskunov, N., et al. 2011, in Solar Polarization 6, ASP Conf. Ser., 437, 237
ud-Doula, A., & Owocki, S. P. 2002, ApJ, 576, 413
Ud-Doula, A., Owocki, S. P., & Townsend, R. H. D. 2009, MNRAS, 392, 1022
Wade, G. A., Maíz Apellániz, J., Martins, F., et al. 2012, MNRAS, 425, 1278
Wade, G. A., Grunhut, J., Alecian, E., et al. 2014, in IAU Symp., 302, 265
Walborn, N. R. 1983, ApJ, 268, 195
Zboril, M., North, P., Glagolevskij, Y. V., & Betrix, F. 1997, A&A, 324, 949

Appendix A: Bonn pipeline output for the FORS2 CPD −62° 2124 data
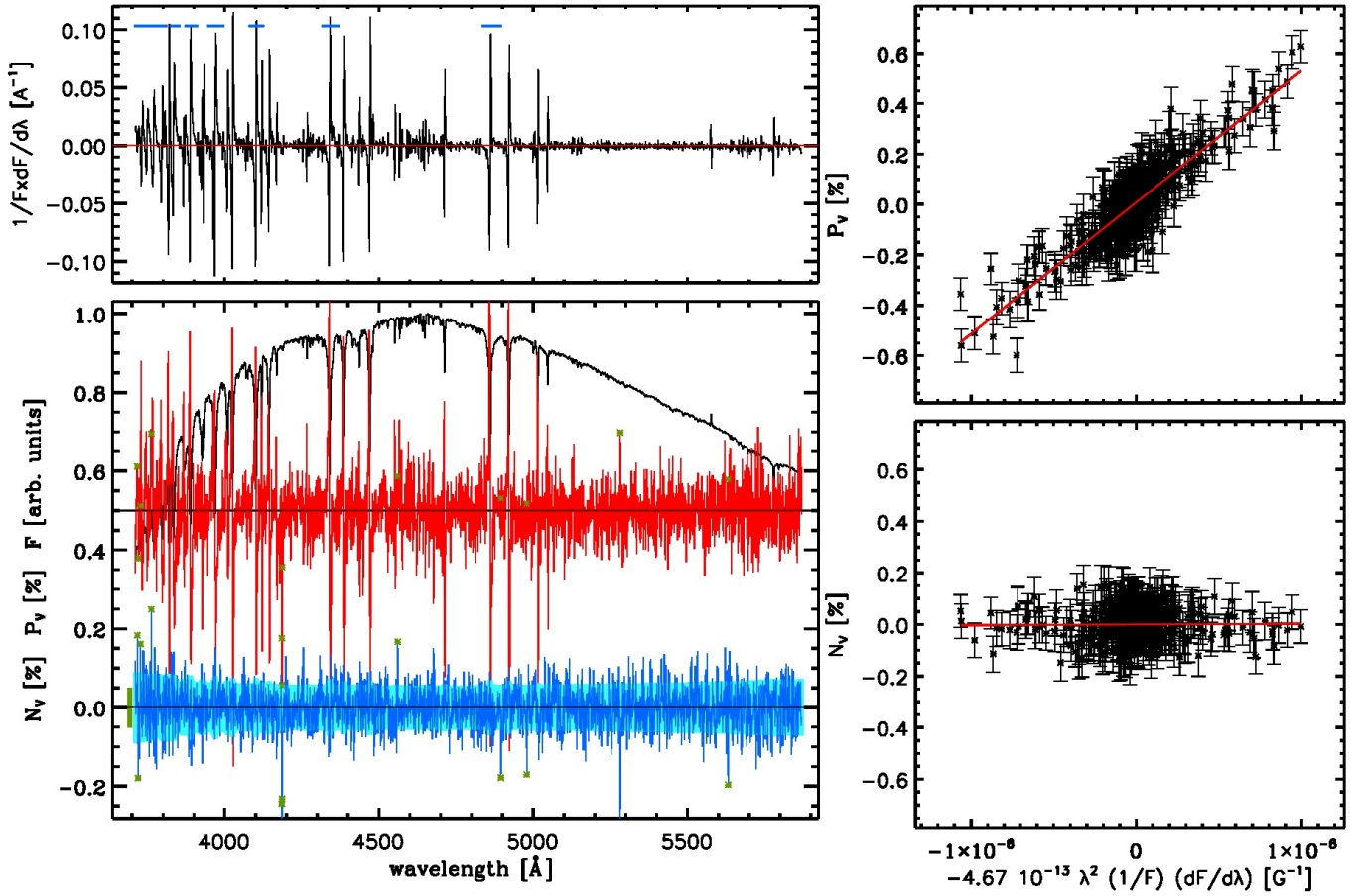
Fig. A.1. Overview of the results of the analysis of the FORS2 data of CPD −62° 2124 using the Bonn pipeline and considering the hydrogen lines. The *top-left panel* shows the derivative of Stokes *I*. The regions used for the calculation of the magnetic field are marked by a thick blue line close to the top of the panel. *Bottom-left panel*: the top profile shows Stokes *I* arbitrarily normalised to the highest value, the middle red profile shows Stokes *V* (in %) shifted upwards for visualisation reasons and the bottom blue profile shows the spectrum of the *N* parameter (in %). The green asterisks mark the points that have been removed by the σ clipping algorithm. The pale blue strip superimposed upon the *N* profile shows the uncertainty associated with each spectral point. The thick green bar on the left side of the spectrum of the *N* parameter shows the standard deviation of the *N* profile. The *top-right panel* shows the linear fit used for the determination of the magnetic field using the Stokes *V* (i.e. $\langle B_z \rangle$). The red solid line shows the best fit. From the linear fit we obtain $\langle B_z \rangle = 5222 \pm 123$ G. The *bottom-right panel* is the same as the bottom-left panel, but for the null profile (i.e. $\langle B_z \rangle$). From the linear fit, we obtain $\langle B_z \rangle = 25 \pm 95$ G.

Appendix B: CPD −62° 2124 HARPSpol stellar atmosphere modelling
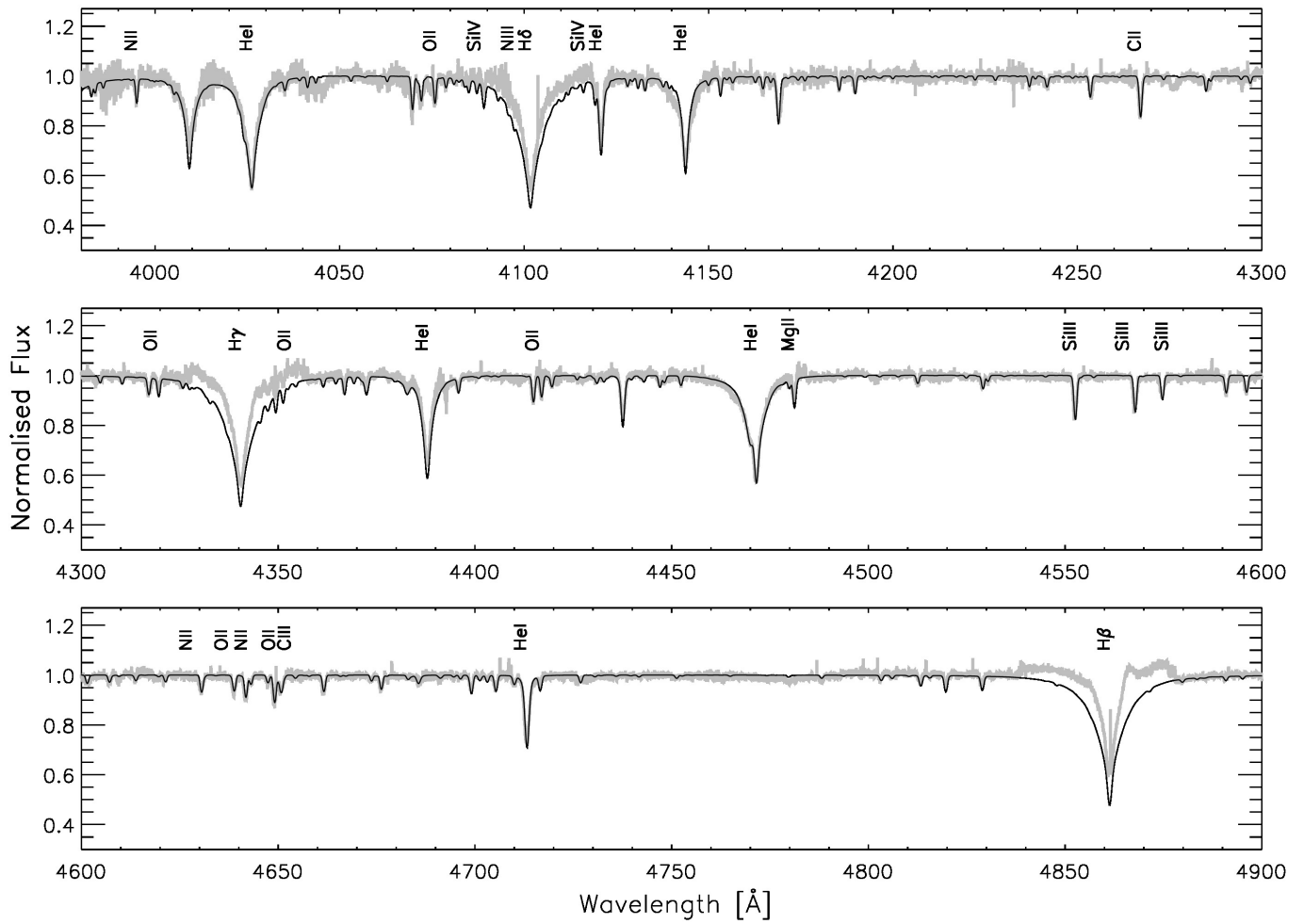
Fig. B.1. Normalised HARPSpol optical spectrum (grey) and the best-fitting stellar model (black). Some of the most prominent features are marked.